Nanoengineering the built-in electric field of a photonic device by interstitial-ion diffusion

A. Nasir,[1] O. Makarovsky,[1] S. Kumar,[2] M. W. Fay,[3] R. Campion,[1] A. Rastelli,[2] O. G. Schmidt,[2] L. Eaves,[1] and A. Patanè[1,*]

[1]*School of Physics and Astronomy, University of Nottingham, Nottingham NG7 2RD, United Kingdom*

[2]*Institute for Integrative Nanosciences, IFW Dresden, D-01069 Dresden, Germany*

[3]*Nottingham Nanotechnology and Nanoscience Centre, University of Nottingham, Nottingham NG7 2RD, United Kingdom*

(Received 22 February 2012; revised manuscript received 4 April 2012; published 17 May 2012)

We use focused laser annealing to activate the diffusion of Mn-interstitial ions (Mn_i^{2+}) from a *p*-(GaMn)As layer towards the intrinsic GaAs/AlAs quantum well (QW) region of a *p-i-n* light emitting diode (LED). The random clustering of the Mn_i^{2+} ions creates a complex potential landscape U and electric field $\mathbf{F}^{Mn} = -\nabla U$ in the QW plane, which we probe with nanoscale precision by monitoring the quantum-confined Stark shift of the "natural" quantum dots formed in the QW. The use of focused laser annealing to form electric field landscapes at predetermined positions is potentially applicable to other material systems containing mobile dopant atoms and is relevant to research on nanophotonics and manipulation of quantum devices.

DOI: 10.1103/PhysRevB.85.195317 PACS number(s): 78.20.−e, 73.22.−f, 78.55.Cr

I. INTRODUCTION

Nanoscale electronic and photonic devices on a single chip could provide an efficient route to integrated photonics. For example, nanolight emitting diodes (nano-LEDs) have potential for use in intra- and interchip optical communications, ultrahigh density optical information storage, and lab-on-a-chip systems. Frontier research in nanophotonics presently requires lithography for the miniaturization of solid-state[1] and soft-matter[2] devices, and/or the growth of low-dimensional structures such as nanowires[3] and quantum dots.[4,5] Recently, laser-induced thermal diffusion of mobile charged dopants into the active region of an LED has been exploited as an alternative means of forming preferential submicron-sized channels for electrical injection of carriers and achieving spatial control of the electroluminescence (EL) emission from the surface of the LED.[6,7] This technique can create a wavelength resolution-limited LED spot at one or more predetermined positions on the crystal surface or else an ordered array of such nano-LEDs. Among dopants in III-V compounds, Mn-interstitial (Mn_i^{2+}) ions in GaAs provide a test bed for this fabrication approach as they are highly mobile double donors.[8–11] Although there is now a large body of indirect experimental evidence for the diffusion of Mn_i across a (GaMn)As/GaAs interface at temperatures $T > 150$ °C, the direct observation of single Mn_i ions remains a lively research topic[8–12] and, only recently, have individual clusters of diffused Mn_i^{2+} ions been revealed by tunneling microscopy.[9] This is partly due to the high level of sensitivity needed to detect low concentrations of Mn_i and the lack of a reliable technique to control the concentration of Mn_i in a heterostructure device containing the ferromagnetic semiconductor (GaMn)As.[13]

To date laser annealing has provided a successful tool for tuning the structural, magnetic, and electronic properties of (GaMn)As.[7,14,15] In Ref. 7 we describe how a focused laser beam can be used to activate the diffusion of Mn-interstitial ions (Mn_i^{2+}) from a (GaMn)As layer towards the intrinsic GaAs/AlAs quantum well (QW) region of a *p-i-n* diode structure thus creating a complex potential landscape U in the (x, y) plane of the QW.[7] Here we probe the random clustering of the Mn_i^{2+} ions induced by the laser annealing by monitoring with nanoscale precision the quantum-confined Stark shift of the "natural" quantum dots formed in the QW plane. The spatially varying electric field $\mathbf{F}^{Mn} = -\nabla U$ associated with this potential acts to reduce significantly the built-in electric field of the *p-i-n* junction in nanoscale regions of the (x, y) plane and leads to the enhancement of the EL emission from spot-like regions of the laser annealed LEDs. The use of focused laser annealing to form nanoscale optical devices and controlled electric field landscapes at predetermined positions in a device is potentially applicable to other material systems containing mobile dopant atoms and could be implemented to locate and tune individual quantum states for applications in quantum information and nanophotonics.[16] These observations also advance research on the electronic properties and device applications of (GaMn)As.[17–20] Although several papers have reported the optical properties of GaAs-based heterostructures doped with Mn,[21–23] the effect of the Mn-interstitial diffusion on the optical properties of natural QDs formed in undoped quantum wells is still unknown.

II. EXPERIMENT

Our samples are *p-i-n* resonant tunnelling LEDs with an AlAs/GaAs/AlAs QW embedded in the intrinsic (i) layer (Fig. 1). These heterostructures were grown by molecular beam epitaxy on (001) n^+-GaAs substrates and have the following layer composition, in order of growth: a 300 nm thick buffer layer of n^+-GaAs, Si-doped to 2×10^{18} cm^{-3}, a 100 nm layer of n-GaAs doped to 2×10^{17} cm^{-3}, an undoped central intrinsic region comprising a 20 nm GaAs spacer layer, a 5 nm AlAs tunnel barrier, a 6 nm GaAs QW, a 5 nm AlAs tunnel barrier, a 10 nm GaAs spacer layer (all grown at 600 °C) and, finally, a 50 nm capping layer of p^+-$Ga_{1-x}Mn_xAs$ with a nominal Mn content of $x = 5\%$, 8%, and 12% grown at 220 °C ($x = 5\%$) and 200 °C ($x = 8\%$, 12%). The LED structure with $x = 5\%$ corresponds to the sample studied in Refs. 6 and 7. Mesa diodes of 200 μm diameter were fabricated by optical lithography with ring-shaped Ti/Au contacts for electrical and optical studies. The setup for microphotoluminescence (μPL) and μEL measurements comprises an optical cryostat mounted on a XY linear positioning stage, an optical microscope equipped with a nanofocusing system, a spectrometer with

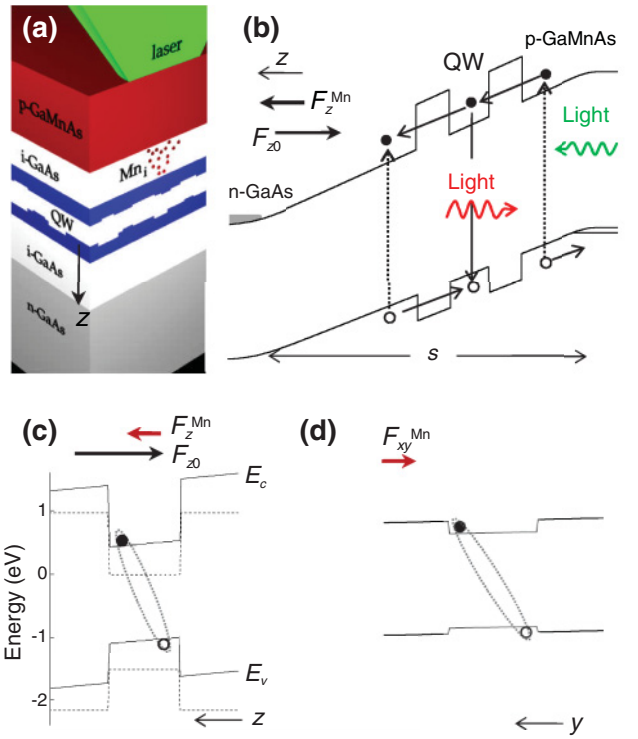

FIG. 1. (Color online) (a) Schematic of our LEDs and of the laser-induced diffusion of Mn_i from the *p*-type (GaMn)As layer towards the AlAs/GaAs/AlAs QW. (b) Schematic of the potential profile and carrier dynamics for an LED with above-band-gap illumination at a bias below the flat-band condition. Photoexcited electrons and holes generated in the undoped GaAs layers on opposite sides of the QW drift towards the QW under the action of the built-in potential in the *p-i-n* junction. They enter the QW by tunneling through the AlAs barriers. Hence, following energy relaxation, they form excitons that become bound in the localized potential minima of the QW. The average built-in electric field at $V = 0$ is F_{z0} and is reduced locally by the electric field F_z^{Mn} created by Mn_i ion clusters. (c) and (d) Schematic of the potential profile of a natural quantum dot and of a bound exciton under the local electric field components F_z^{Mn} and F_{xy}^{Mn}. The continuous line in (c) represents the calculated energy band diagram at $V = 0$ V ($F_{z0} = -272$ kV/cm) and $F_z^{Mn} = +100$ kV/cm. The dashed line shows the band diagram at flat bands.

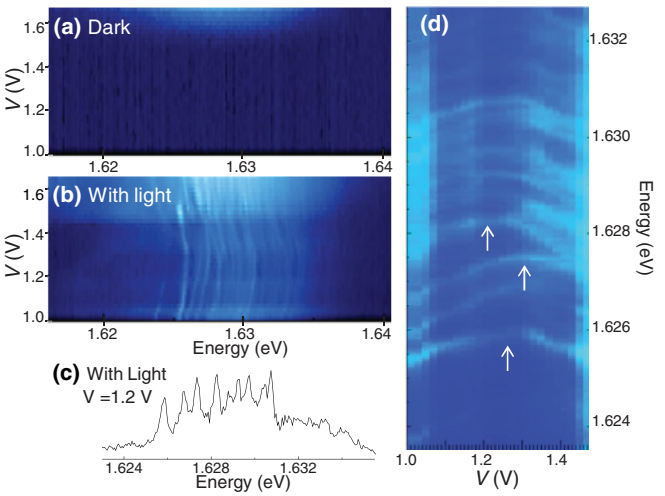

FIG. 2. (Color online) Color maps of the photon emission intensity vs bias and photon energy (a) without and (b) with light illumination with a laser beam of diameter $d = 1$ μm, $\lambda = 532$ nm, and $P = 100$ nW at $T = 5$ K for an LED with $x = 5\%$. A selected spectrum taken at $V = 1.2$ V under illumination is shown in (c). (d) Bias dependence of the narrow emission lines. The arrows identify lines whose energy is peaked at different bias values.

0.5 m focal length equipped with a liquid-nitrogen cooled charge coupled device (CCD), and a low-noise (<0.1 pA) electrical transport measurement system. A frequency-doubled Nd:YVO_4 laser ($\lambda = 532$ nm) or an Ar laser ($\lambda = 515$ nm) were used for the laser annealing studies.

III. RESULTS AND DISCUSSION

Recently we investigated the effects of the laser annealing on the EL emission of the QW and GaAs layers and showed that by annealing a small spot with a focussed laser beam it is possible control the local electrostatic potential in the QW plane and create a preferential path for charged carriers. In turn, this activates a nanoscale region of the LED to emit light at an applied bias well below the threshold voltage for emission from the nonannealed regions.[6,7] Here we focus on the μPL emission of the natural QDs formed in the QW plane, its dependence on the applied bias in the annealed and nonannealed LEDs and what it tells us about the electrostatic potential landscape arising from diffused Mn_i^{2+} ions.

The bias dependence of the low temperature ($T = 5$ K) μEL of a nonannealed LED with a $Ga_{1-x}Mn_xAs$ layer containing 5% Mn is shown as a color scale plot in Fig. 2(a): the QW EL emission band is centered at 1.63 eV and is observed above a threshold bias, $V \geqslant 1.5$ V. The effect on the QW emission spectrum of illumination with low intensity ($P = 100$ nW) laser light of wavelength $\lambda = 532$ nm is illustrated in Figs. 2(b) and 2(c). We note that this laser power is too low to cause any irreversible change of the sample due to annealing-induced diffusion of Mn_i ions. The laser illumination gives rise to sharp (~500 μeV) PL emission peaks not only at $V > 1.5$ V, but also at much lower voltages. As illustrated in Fig. 1(b), at low applied bias voltages, photoexcited electrons and holes generated in the undoped GaAs layers on opposite sides of the QW can drift toward the QW under the action of the built-in potential in the *p-i-n* junction. They enter the QW by tunneling through the AlAs barriers. Hence, following energy relaxation, they form excitons that become bound in the localized potential minima of the QW. These minima, also called *natural* quantum dots, arise from monolayer fluctuations in the well-width and other disorder-related effects.[24–26] The resulting sharp spectral lines are highly reproducible, but tend to merge into a broader continuum band at high laser excitation powers due to state filling. Note that the observation of these sharp excitonic lines requires the presence of light illumination, that is, they are not observed in the EL spectra since holes cannot be electrically injected from the *p*-(GaMn)As layer into the QW in the absence of light illumination and at biases below the flat-band condition.

The emission energy of the narrow PL lines is strongly sensitive to the applied bias due to the quantum-confined Stark

effect.[24–26] A Stark shift can arise from the effect of both the normal (along z) and in-plane components of the local electric field $\mathbf{F}$ on the bound excitonic states. We can control the strength of the normal electric field component by means of the applied bias voltage. From the plot in Fig. 2(d), it can be seen that the bias-induced Stark shift of each sharp line j reaches a maximum at a slightly different value of the applied bias V_j. However, the energy shifts of all the lines ΔE_j are similar in magnitude and can be described by a quadratic electric field dependence of the type $\Delta E_j = -\beta[(V - V_j)/s]^2 = -\beta F_{jz}^2$. Here $F_{jz} = (V - V_j)/s$ is the bias-dependent electric field component along z characteristic of line j, $s = 46$ nm is the separation between the n- and p-type contact layers and β is the polarizability of the excitonic state. We find that β has a similar value for all peaks ($\beta/e = 21 \pm 4$ nm^2/V). Thus we conclude that the different values of V_j arise from local variations (on length scales smaller than our laser spot size, i.e., 1 μm) of the built-in potential in the plane of the QW rather than from differences in the polarizability of the exciton along the z direction. The average value of V_j is $\bar{V}_j = V_0 = 1.25 \pm 0.03$ V, corresponding to a built-in electric field $F_{z0} = V_0/s = -272 \pm 7$ kV/cm, which is directed from the n to the p layer of the p-i-n junction [Fig. 1(b)].

In situ focused laser annealing of the LED leads to an enhancement of the QW EL emission from the annealed spot[7] and to the appearance of additional narrow (<1 meV) excitonic lines on the low energy side of the QW PL emission. This is illustrated in Figs. 3(a)–3(d) for a second LED structure with a higher nominal content of Mn, $x = 12\%$, in the p^+-$Ga_{1-x}Mn_xAs$ layer: this creates a high concentration (~2%) of Mn-interstitial ions in the p^+ layer, which can diffuse into the intrinsic region when the device is annealed.[8,13] The color plots of Figs. 3(a)–3(c) show the QW μPL emission intensity versus applied bias V and photon energy before [Figs. 3(a) and 3(b)] and after [Fig. 3(c)] annealing with a focused laser beam of diameter $d = 1$ μm, $\lambda = 532$ nm and annealing laser power $P_a = 205$ mW at $T = 5$ K. The narrow lines that emerge following laser annealing can be as deep as 10–30 meV below the main QW PL band [see peaks p_1, p_2, and p_3 in Figs. 3(c) and 3(d)]. Although the parabolic Stark shifts of these excitonic lines have the same curvature as that for the nonannealed samples (i.e., $\Delta E_j = -\beta F_{jz}^2$ with the same $\beta/e = 21 \pm 4$ nm^2/V), we observe a significant difference in the bias values of their maxima [see Fig. 3(e)]. For the annealed samples, the maxima for the excitonic lines in the spectroscopic region of the main QW band are still at $V_0 = 1.25 \pm 0.03$ V, which corresponds to a built-in electric field of $F_{z0} = -272 \pm 7$ kV/cm. In contrast, for the excitonic lines induced by the laser annealing, the maxima of the parabola are shifted at significantly lower bias voltages, corresponding to local built-in electric fields $F_{jz0} = -V_j/s = -122$, -152, and -260 kV/cm for lines p_1, p_2, and p_3, respectively. We have observed similar lines in the laser-annealed spots of several other devices. We therefore conclude that the modified Stark shift of this group of lines is due to thermal diffusion of Mn_i^{2+} from the $Ga_{1-x}Mn_xAs$ layer into the underlying undoped GaAs layer. The randomly distributed ionized Mn_i^{2+} donors create a varying electrostatic potential U in the QW plane and a corresponding strong electric field $\mathbf{F}^{Mn}$. The mesoscopic fluctuations in the normal

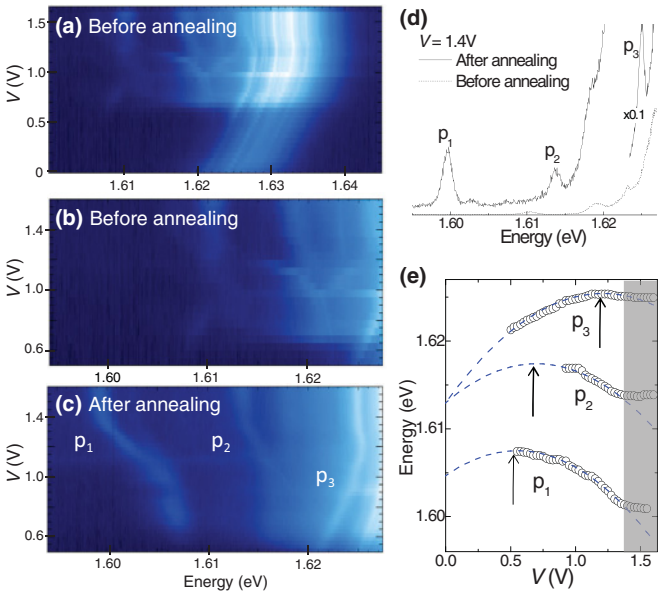

FIG. 3. (Color online) Color maps of the photon emission intensity vs bias and photon energy (a) and (b) before and (c) after laser annealing with a focused laser beam of diameter $d = 1$ μm, $\lambda = 532$ nm, and $P_a = 205$ mW at $T = 5$ K for an LED with $x = 12\%$. The measurement was performed at $T = 5$ K with a low power excitation ($P = 100$ nW, $\lambda = 532$ nm). The optical spectra at $V = 1.4$ V are shown in (d). (e) Bias dependence of three narrow optical lines p_1, p_2, and p_3 induced by laser annealing. The saturation of the bias dependence of the lines for biases above the flat-band condition (see shaded area) is caused by screening effects due to the large forward bias current. The arrows identify lines whose energy is peaked at different bias values.

component F_z^{Mn} can significantly reduce locally the built-in electric field of the p-i-n junction and accounts for the observed variation of the F_{jz0} values derived from the Stark shifts. Our measured values of F_{jz0} indicate that Mn_i clusters can induce fields F_z^{Mn} of up to $+150$ kV/cm (for line p_1).

We model these electrostatic effects by describing the diffusion of Mn_i^{2+} along the growth direction z in terms of a one-dimensional model based on Fick's Law, that is, $C(z,t) = C_s \mathrm{erfc}(z/2\sqrt{Dt_A})$.[8] Here C is the concentration of Mn_i^{2+} at a distance z below the $Ga_{1-x}Mn_xAs$/GaAs interface, $t_A = 1$ s is the annealing time, $C_s \approx 10^{20}$ cm^{-3} is the concentration of Mn_i^{2+} in the $Ga_{1-x}Mn_xAs$ layer (for $x = 12\%$, 2% of Mn atoms occupy interstitial positions),[13] $D = D_0 \exp(-Q/k_B T_A)$ is the Mn_i^{2+} diffusion coefficient, $D_0 = 3 \times 10^{-4}$ m^2/s, $Q = 1.5$ eV is the activation energy[8,10] and T_A is the annealing temperature, which we calculate using the temperature-dependent thermal conductivity and optical absorption coefficient at $\lambda = 532$ nm of GaAs.[27,28] For the numerical simulation of the electrostatic potential U we use 2×10^6 Mn_i^{2+} ions occupying a volume of $1.4 \times 1.4 \times d$ μm^3, where $d = 18$ nm is the distance of the central plane of the QW from the $Ga_{1-x}Mn_xAs$/GaAs interface.

As shown in Fig. 4(a), the simulated potential energy $U(x, y)$ in the central plane of the QW exhibits deep potential minima with typical depths of ~0.1 eV and width of ~10 nm, corresponding to QW regions close to clusters of Mn_i^{2+} ions.

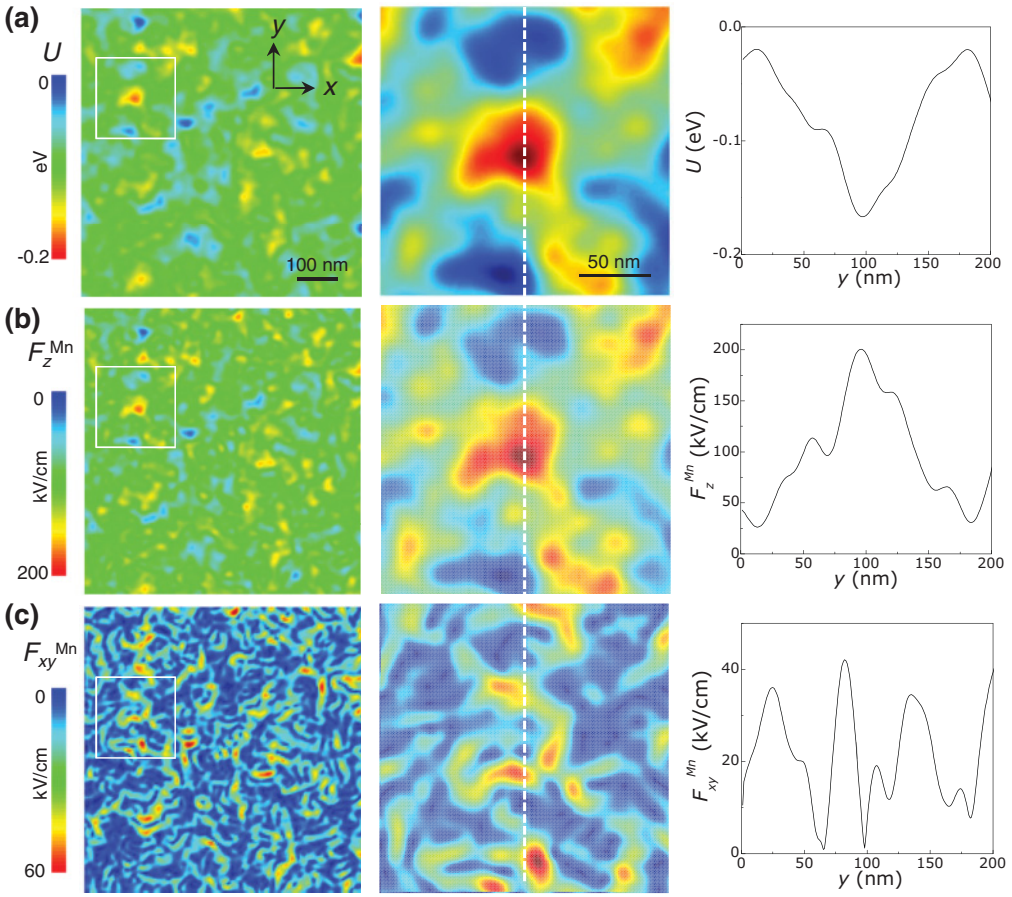

FIG. 4. (Color online) Numerical simulations of (a) the electrostatic potential $U(x,y)$ and (b) and (c) electric field components F_z^{Mn} and F_{xy}^{Mn} created in the central plane of the QW by Mn_i ions. The squares on the left are magnified in the middle panels. The dependence of U, F_z^{Mn}, and F_{xy}^{Mn} on y, along the dotted lines in the middles maps, is illustrated in the right panels.

These minima create an attractive potential for electrons and induce a large local electric field component $F_z^{Mn}(x,y)$ along the growth direction z, of up to $\sim +200$ kV/cm [see Fig. 4(b)] in good agreement with the strength of electric field F_z^{Mn} (up to +150 kV/cm) deduced from our spectroscopic data. Thus our observation of Stark-shifted bound exciton emission lines at bias voltages as low as $V = 1$ V provides spectroscopic evidence for the significant reduction of the built-in electric field of the *p-i-n* junction by the Mn_i^{2+} clusters formed at the laser-annealed spots. Our simulation also indicates that around each minimum in $U(x, y)$ the direction and magnitude of the in-plane electric field component $F_{xy}^{Mn}(x,y) = \sqrt{F_x^2+F_y^2}$ can fluctuate strongly, by up to 60 kV/cm, see Fig. 4(c). This field component induces the excitons localized on the *natural* quantum dots to become spatially "indirect", that is, the bound excitons acquire a permanent in-plane electric dipole moment $p_{xy} = er$, where the electron-hole spatial separation r and the direction of the dipole vary in the (x, y) plane [Figs. 1(c) and 1(d)]. This can explain why the additional excitonic lines (e.g., p_1, p_2, p_3) in the QW emission spectrum of the laser-annealed LEDs appear at lower energies relative to the main QW PL peak and why those lines that are peaked at lower energies are also more significantly shifted in bias [see Fig. 3(d)]. We use the energy shift ΔE of the parabola relative to the QW peak at flat band to estimate r: for $\Delta E = -p_{xy}F_{xy}^{Mn} =$ -10 to -20 meV and $F_{xy}^{Mn} = 60$ kV/cm, we obtain $r = p_{xy}/e = 2$ to 4 nm. This range of values indicates a relatively large electric field-induced electron-hole separation in the QW plane, consistent with the previously observed weak in-plane confinement of excitons in these *natural* quantum dots.[25]

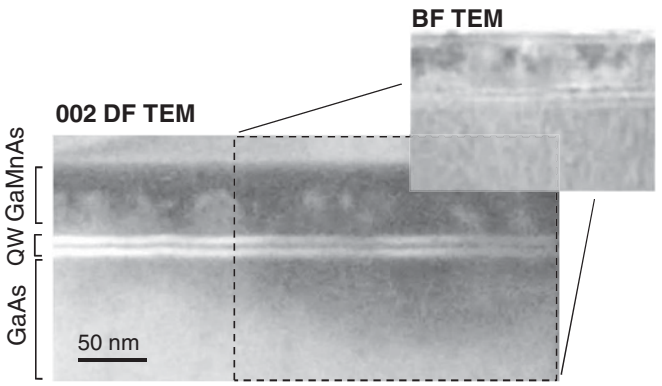

FIG. 5. (002) dark field and bright field TEM images of a 250 nm thick lift-out cross section of a laser annealed LED with 5% Mn. The dashed rectangle in the main figure identifies a region closer to the laser annealed spot. The LED was annealed using a focused laser beam of diameter $d = 1$ μm, wavelength $\lambda = 515$ nm, and power $P_a = 40$ mW at $T = 300$ K.

Our optical data and analysis are supported by microscopic (002) dark field (DF) transmission electron microscopy (TEM) measurements. In the (002) DF TEM imaging mode, the (002) diffracted beam intensity is very sensitive to the local concentration of Mn interstitials since the structure factor is not affected strongly by substitutional Mn-acceptor ions, but is reduced by the energetically favored type-2 interstitials, that is, Mn interstitials surrounded by four As nearest neighbors.[29] Close to the laser-annealed spot, the (002) DF cross sectional TEM images of our LEDs show darker intensity regions both above and below the QW (see the dashed rectangle in Fig. 5). This contrast is not observed in the nonannealed areas of the DF TEM image and is absent in the bright field TEM images (inset of Fig. 5),[30] consistent with it originating from diffusion of Mn interstitials out of the $Ga_{1-x}Mn_xAs$ layer into the underlying undoped GaAs layers and toward the GaAs/AlAs QW. The diffusion of Mn interstitials and the corresponding reductions of the electric field in nanoscale regions of the *p-i-n* diode explain the changes observed in the emission spectra of our laser-annealed devices (see Fig. 3) and why focused laser annealing can enhance the electroluminescence emission of the LED from nanoscale regions and at applied voltages below the flat-band condition.[7]

IV. CONCLUSION

In conclusion, the quantum-confined Stark shift of the localized excitonic emission lines in a quantum well provides us with a nanoscale probe of the strength of the electric field induced in the well by the laser-induced diffusion of Mn-interstitial ions. Our findings demonstrate that these highly mobile ions can be used to modify locally the built-in electric field at predetermined locations, a phenomenon which can be exploited to produce diffraction-limited light-emitting spots at selected points on the surface of a photonic device[7,17] and to induce controlled changes in the quantum properties of individual nanostructures for quantum information technology.[26] Laser-induced manipulation could be applied to other functional materials containing highly mobile atomic species and advance the fabrication and manipulation of nanoscale electronic devices.

ACKNOWLEDGMENTS

This work was supported by The Royal Society, the DFG (FOR730), and the BMBF (QK_QuaHL_Rep, project 01BQ1032).

*Corresponding author: amalia.patane@nottingham.ac.uk

[1] H. W. Choi, C. W. Jeon, C. Liu, I. M. Watson, M. D. Dawson, P. R. Edwards, R. W. Martin, S. Tripathy, and S. J. Chua, Appl. Phys. Lett. **86**, 021101 (2005).

[2] H. Yamamoto, J. Wilkinson, J. P. Long, K. Bussman, J. A. Christodoulides, and Z. H. Kafafi, Nano Lett. **5**, 2485 (2005).

[3] X. Duan, Y. Huang, Y. Cui, J. Wang, and C. M. Lieber, Nature (London) **409**, 66 (2001).

[4] E. D. Minot, F. Kelkensberg, M. van Kouwen, J. A. van Dam, L. P. Kouwenhoven, V. Zwiller, M. T. Borgstrom, O. Wunnicke, M. A. Verheijen, and E. P. A. M. Bakkers, Nano Lett. **7**, 367 (2007).

[5] A. Baumgartner, E. Stock, A. Patanè, L. Eaves, M. Henini, and D. Bimberg, Phys. Rev. Lett. **105**, 257401 (2010).

[6] F. Intonti, V. Matarazzo, A. Nasir, O. Makarovsky, R. Campion, A. Patanè, S. Kumar, A. Rastelli, O. G. Schmidt, and M. Gurioli, Appl. Phys. Lett. **98**, 183102 (2011).

[7] O. Makarovsky, S. Kumar, A. Rastelli, A. Patanè, L. Eaves, A. G. Balanov, O. G. Schmidt, R. Campion, and C. T. Foxon, Adv. Mater. **22**, 3176 (2010).

[8] K. W. Edmonds, P. Boguslawski, K. Y. Wang, R. P. Campion, S. N. Novikov, N. R. S. Farley, B. L. Gallagher, C. T. Foxon, M. Sawicki, T. Dietl, M. Buongiorno Nardelli, and J. Bernholc, Phys. Rev. Lett. **92**, 037201 (2004).

[9] A. P. Wijnheijmer, O. Makarovsky, J. K. Garleff, L. Eaves, R. P. Campion, B. L. Gallagher, and P. M. Koenraad, Nano Lett. **10**, 4873 (2010).

[10] O. Makarovsky, A. G. Balanov, L. Eaves, A. Patané, R. P. Campion, C. T. Foxon, and R. J. Airey, Phys. Rev. B **81**, 035323 (2010).

[11] T. Jungwirth *et al.*, Phys. Rev. B **72**, 165204 (2005).

[12] L. M. C. Pereira, U. Wahl, S. Decoster, J. G. Correia, M. R. de Silva, A. Vantomme, and J. P. Araujo, Appl. Phys. Lett. **98**, 201905 (2011).

[13] T. Jungwirth, J. Sinova, J. Masek, J. Kucera, and A. H. McDonald, Rev. Mod. Phys. **78**, 809 (2006).

[14] R. Farshchi and O. D. Dubon, D. J. Hwang, N. Misra, C. P. Grigoropoulos, and P. D. Ashby, Appl. Phys. Lett. **92**, 012517 (2008).

[15] D. Bürger, S. Zhou, M. Pandey, C. S. Viswanadham, J. Grenzer, O. Roshchupkina, W. Anwand, H. Reuther, V. Gottschalch, M. Helm, and H. Schmidt, Phys. Rev. B **81**, 115202 (2010).

[16] T. C. Chong, M. H. Hong, and L. P. Shi, Laser Photon. Rev. **4**, 123 (2010).

[17] S. Ohya, K. Takata, and M. Tanaka, Nat. Phys. **7**, 342 (2011).

[18] C. M. Jaworski, J. Yang, S. Mack, D. D. Awschalom, J. P. Heremans, and R. C. Myers, Nat. Mater. **9**, 898 (2010).

[19] M. Sawicki, D. Chiba, A. Korbecka, Y. Nishitani, J. A. Majewski, F. Matsukura, T. Dietl, and H. Ohno, Nat. Phys. **6**, 22 (2010).

[20] Y. Ohno, D. K. Young, B. Beschoten, F. Matsukura, H. Ohno, and D. D. Awschalom, Nature (London) **402**, 792 (1999).

[21] M. Poggio, R. C. Myers, N. P. Stern, A. C. Gossard, and D. D. Awschalom, Phys. Rev. B **72**, 235313 (2005).

[22] I. F. Sapega, O. Brandt, M. Ramsteiner, K. H. Ploog, I. E. Panaiotti, and N. S. Averkiev, Phys. Rev. B **75**, 113310 (2007).

[23] B. Plot, B. Deveaud, B. Lambert, A. Chomette, and A. Regreny, J. Phys. C **19**, 4279 (1986).

[24] H. F. Hess, E. Betzig, T. D. Harris, L. N. Pfeiffer, and K. W. West, Science **264**, 1740 (1994).

[25] W. Heller, U. Bockelmann, and G. Abstreiter, Phys. Rev. B **57**, 6270 (1998).

[26] S. Marcet, K. Ohtani, and H. Ohno, Appl. Phys. Lett. **96**, 101117 (2010).

[27] M. Lax, J. Appl. Phys. **48**, 3919 (1977).

[28] J. S. Blakemore, J. Appl. Phys. **53**, R123 (1982).

[29] F. Glas, G. Patriarche, L. Largeau, and A. Lemaître, Phys. Rev. Lett. **93**, 086107 (2004).

[30] M. W. Fay, A. Nasir, O. Makarovsky, A. Rastelli, L. Eaves, R. Campion, C. T. Foxon, and A. Patanè, J. Phys. Conf. Ser. **326**, 012055 (2011).